Optik 127 (2016) 259–262

Contents lists available at ScienceDirect

Optik

journal homepage: www.elsevier.de/ijleo

Low-pass spatial filters with small angle-domain bandwidth based on one-dimensional metamaterial photonic crystals

Zhaoming Luo [a,b,*], Min Chen [a], Jiyuan Deng [a], Ying Chen [b], Jing Liu [a]

[a] College of Information and Communication Engineering, Hunan Institute of Science and Technology, Yueyang 414006, China
[b] Key Laboratory for Micro-/Nano-Optoelectronic Devices of Ministry of Education, College of Physics and Microelectronic Science, Hunan University, Changsha 410082, China

ARTICLE INFO

Article history:
Received 18 December 2014
Accepted 10 October 2015

Keywords:
Spatial filter
Metamaterial
Zero-index gap

ABSTRACT

By using the spatial properties of zero-index gaps in one-dimensional metamaterial photonic crystals, we have designed low-pass spatial filters with small angle-domain bandwidth less than 10 degrees. It is demonstrated by transfer matrix method that the small angle-domain bandwidth and roll-off factor of the spatial filters can be adjusted by changing the structure parameters of the metamaterial photonic crystals. In addition, the spatial filters have absolute polarization-independent properties compared with previous photonic crystal spatial filters. These spatial filters with small angle-domain bandwidth may be applied to the laser science in the future, and decrease the space occupied by the traditional spatial filters.

1. Introduction

Low-pass spatial filters have been widely applied to image enhancement and information processing in several regions of the electromagnetic spectrum, particularly in laser science [1–3]. A simple and traditional low-pass spatial filter consists of two focusing lenses in a confocal arrangement and a pinhole in the focus plane, and its angle-domain bandwidth can be tuned by changing the size of the pinhole. The setup, although widely used, has a considerable size (at least four focal lengths) and high standard for the quality and installation of the lens. To overcome the deficiencies of traditional spatial filters, some modern spatial filters are performed based on conventional photonic crystals (PCs) with positive-index materials (PIMs) [4–10]. The application of the spatial filters such as beam smoothing has been demonstrated [7,9,10], but the angle-domain bandwidth of the PC spatial filters is very big compared to the requirements of the laser science [11,12].

Recently, metamaterials have been realized including single-negative (SNG) materials, negative-index materials (NIMs) and zero-index materials (ZIMs), and attract intensive studies due to their unique electromagnetic properties and potential applications [13–24]. With metamaterials being introduced into PCs, three new kinds of gaps have been identified: the zero-average-index gap, the zero-effective-phase gap and the zero-index gap [22–24]. In contrast to Bragg gap, originating from interference mechanisms, it is the material dispersion of the metamaterials that mainly determines the appearances of these new gaps [25]. The zero-average-index gap appears in one-dimensional (1D) PC structures combining PIMs and NIMs, and the zero-effective-phase gap emerges in 1D PC structures containing two different SNG materials. Based on the unique properties of the two gaps, the performances of some frequency filters and spatial filters are improved [22–29]. The zero-index gap is more special and appears near frequencies where the index equals to zero. Different from the former two gaps, it possesses many excellent properties. Thus, we have reason to expect to design a new spatial filter based on the zero-index gap to improve the performance of the PC spatial filters.

In this paper, we aim to test the feasibility of designing low-pass spatial filters with small angle-domain bandwidth based on 1D metamaterial PC structures. Firstly, we investigate the properties of the zero-index gap in detail. Secondly, a practical design is presented based on the gap properties of the zero-index gap. Finally, we summarize the properties of the spatial filters including polarization, angle-domain bandwidth and roll-off factor.

2. Computations model and numerical method

The 1D metamaterial PC structure $(AB)^N$ is shown in Fig. 1 with A and B indicating metamaterial layers. We use a transmission line model to describe the metamaterials that are [17,22,28]

$$\varepsilon_a = \varepsilon_1, \quad \mu_a = \mu_1 - \frac{\omega_{mp}^2}{\omega^2}, \tag{1}$$

* Corresponding author at: College of Information and Communication Engineering, Hunan Institute of Science and Technology, Yueyang 414006, China.
Tel.: +86 15273033069.
E-mail address: zhaomingluo@hnu.edu.cn (Z. Luo).

http://dx.doi.org/10.1016/j.ijleo.2015.10.034
0030-4026/

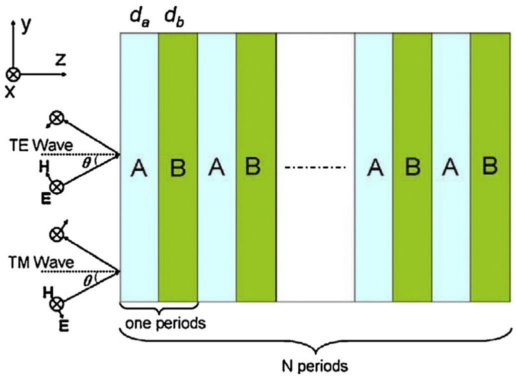

Fig. 1. Schematic of the 1D metamaterial PC structure of $(AB)^N$. A and B indicate metamaterials, and the physical thicknesses of A and B are d_a and d_b.

In metamaterial layer A and

$$\varepsilon_b = \varepsilon_2 - \frac{\omega_{ep}^2}{\omega^2}, \quad \mu_b = \mu_2, \tag{2}$$

In metamaterial layer B, where ω_{mp} and ω_{ep} are the magnetic plasma frequency and electronic plasma frequency respectively. In Eqs. (1) and (2), ω is the angular frequency measured in GHz. The model is introduced to study the metamaterial properties and applications [22–29]. It is noticed that A is the ZIM at specified frequency $\omega = \frac{\omega_{mp}}{\sqrt{\mu_1}}$ and B at $\frac{\omega_{ep}}{\sqrt{\varepsilon_2}}$.

We use the transfer-matrix method [22–29] to analyze the transmittance properties of the 1D metamaterial PC structures. If we inject a plane wave into the 1D metamaterial PC structures at an angle θ in the +z direction, the electric component and magnetic component for the qth layer can be related via a transfer matrix,

$$M_q = \begin{pmatrix} \cos\beta_q & -\dfrac{i}{p_q}\cos\beta_q \\ -ip_q\cos\beta_q & \cos\beta_q \end{pmatrix} \tag{3}$$

where $\beta_q = (2\pi/\lambda)\sqrt{\varepsilon_q}\sqrt{\mu_q}d_q$, $p_q = \sqrt{\varepsilon_q/\mu_q}\sqrt{1-\sin^2\theta/(\varepsilon_q\mu_q)}$ for TE polarization and $p_q = \sqrt{\mu_q/\varepsilon_q}\sqrt{1-\sin^2\theta/(\varepsilon_q\mu_q)}$ for TM polarization with ε_q, μ_q, d_q, and λ being, respectively, the relative permittivity, the relative permeability, the physical thickness of the qth layer and the wavelength of the incident wave.

The transmission matrix of the whole structure can be written as

$$M = \prod M_j(d_j, \omega) = \begin{pmatrix} x_{11} & x_{12} \\ x_{21} & x_{22} \end{pmatrix} \tag{4}$$

and the reflectivity and transmissivity are derived out to be [28]

$$R = \left|\frac{(x_{11}+p_s x_{12})p_0 - (x_{21}+p_s x_{22})}{(x_{11}+p_s x_{12})p_0 + (x_{21}+p_s x_{22})}\right|^2, \tag{5}$$

$$T = \frac{p_s}{p_0}\left|\frac{2p_0}{(x_{11}+p_s x_{12})p_0 + (x_{21}+p_s x_{22})}\right|^2, \tag{6}$$

where $p_0 = p_s = \sqrt{1-\sin^2\theta/(\varepsilon_0\mu_0)} = \cos\theta$ for the vacuum ($\varepsilon_0 = \mu_0 = 1$) at the left- and right-hand side of the structure.

3. Results and discussion

We first investigate the gap properties of the metamaterial PCs $(AB)^N$ as shown in Fig. 1, and choose the structure parameters as follows: $\varepsilon_1 = 2$, $\mu_1 = 1$, $\varepsilon_2 = 1$, $\mu_2 = 2$, $\omega_{ep} = \omega_{mp} = \omega_p = 10/(2\pi)$ GHz, $N = 8$. According to the structure parameters, A and B are both ZIMs at specified frequency $\omega = \omega_p$. In the frequency range of $\omega > \omega_p$, all ε and μ are positive. That is to say, A and B are both PIMs. The SNG materials including the mu-negative (MNG) and epsilon-negative (ENG) materials correspond to the frequency range of $\omega < \omega_p$, with A being MNG materials and B ENG materials. The transmittance spectra of the 1D metamaterial PC structure with the incident angles $\theta = 0°$, 30°, 60° and 85° are shown in Fig. 2(a). It can be seen that the Bragg gap emerges in the double-positive frequency range and the zero-effect-phase gap in the single negative frequency range. Meanwhile, the zero-index gap also arises near the zero-index frequency. In order to observe the zero-index gap distinctly, Fig. 2(a) is redrawn in the frequency range from 0.5 GHz to 2.5 GHz (see Fig. 2(b)). It is clearly shown that there is no gap beside the zero-index frequency ($\omega_p \approx 1.592$ GHz) at normal incidence, and the zero-index gap emerges and becomes wider and wider with the increase of the incident angle. Thus we can conclude that the zero-index gap is very sensitive to the incident angles. Such a result is due to the breaking of Snell's law when the refractive index n satisfies the condition of $0 \le n \le 1$, that is to say, no real solution for any refraction angle θ_r of the equation $\sin\theta = n_r \sin\theta_r$ (r = A or B) under the inclined incident angle ($\theta \ne 0$) [23]. In the above discussion, we have considered the gap properties of the structure for TE polarization. We also calculate the transmittance spectra of the structure for TM polarization, as shown in the dashed curve of Fig. 2(b). It is seen that the two curves for TE and TM polarization are overlapped. Thus the gap is polarization-independent, which is the reason that the structure has good electromagnetic symmetry [30].

The conclusion from the above analysis that the zero-index gap is sensitive to the incident angle is a prerequisite for the realization of spatial filters with small angle-domain bandwidth. We next design a new low-pass spatial filter based on the spatial properties

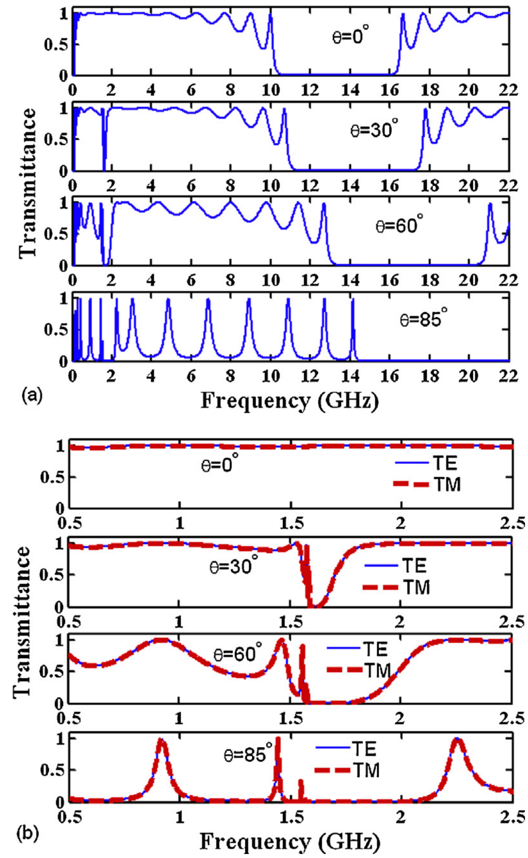

Fig. 2. Transmittance spectra of the 1D metamaterial PC structure of $(AB)^8$ at the different incident angles $\theta = 0°$, 30°, 60° and 85°. (b) is the part of (a). The blue solid (red dashed) curves are for TE (TM) polarization. Structure parameters: $\varepsilon_1 = 2$, $\mu_1 = 1$, $\varepsilon_2 = 1$, $\mu_2 = 2$, $\omega_{ep} = \omega_{mp} = \omega_p = 10/(2\pi)$ GHz. (For interpretation of the references to color in this figure legend, the reader is referred to the web version of this article.)